12 Mar 1991, 10:30 am - 12:00 pm

Effective Stress Analysis of a Sheet Pile Quaywall

Susumu Iai
Port and Harbour Research Institute, Ministry of Transport, Japan

Tomohiro Kameoka
Port and Harbour Research Institute, Ministry of Transport, Japan

Proceedings: Second International Conference on Recent Advances in Geotechnical Earthquake Engineering and Soil Dynamics, March 11-15, 1991, St. Louis, Missouri, Paper No. 4.14

Effective Stress Analysis of a Sheet Pile Quaywall

Susumu Iai
Port and Harbour Research Institute, Ministry of Transport, Japan

Tomohiro Kameoka
Port and Harbour Research Institute, Ministry of Transport, Japan

SYNOPSIS In 1983, Nihonkai Chubu Earthquake of magnitude 7.7 hit northern part of Japan. The earthquake caused damage to quaywalls at Akita Port located about 100 km from the epicenter. The damage was associated with the liquefaction of backfill sand. In order to analyze the mechanism of the damage, soils are taken from the site for laboratory tests. The record of the earthquake motion is digitized. Based on these investigations, a two dimensional effective stress analysis is conducted. The model used in this study consists of a multiple virtual simple shear mechanisms oriented in arbitrary directions. The results of the effective stress analysis indicate that a fundamental mechanism in producing deformation of the soil and the structure is due to the initial stress and its release in accordance with the progress of cyclic mobility. This mechanism of deformation is quite different from that indicated by the conventional Newmark's sliding block concept.

INTRODUCTION

Serious damage to the sheet pile quaywalls during earthquakes is known to be associated with liquefaction or cyclic mobility of backfill sand. The detailed mechanism of the deformation, however, is not very well understood at present. The deformation is usually limited to some degree, indicating that in most of the cases the cyclic mobility is the main cause of the deformation of the sheet pile quaywalls during earthquakes. Though Newmark's sliding block concept is often adopted as a convenient and simple tool for estimating the earthquake induced deformation of soil structures, the concept of sliding is not consistent with the mechanism of cyclic mobility of saturated soil, in which soil never involves the complete failure of soil.

In order to understand the mechanism of the deformation of anchored sheet pile quaywalls during earthquakes, the effective stress analysis is conducted in the present study. As a case history data to be studied, the damage at Akita Port during 1983 Nihonkai Chubu Earthquake of magnitude 7.7 in Japan is chosen. Akita Port is located about 100 km from the epicenter as shown in Fig. 1, shaken by the earthquake motion with the maximum acceleration of 205 Gals.

OUTLINE OF THE MODEL

The constitutive model used for the present study is composed of two parts; a stress-strain relation for shear mechanism and a mechanism for generating excess pore water pressure. The theoretical framework is of the generalized strain space plasticity - multiple mechanism type (Iai, 1991).

In this approach, the stress-strain relation for shear mechanism is idealized, as shown in

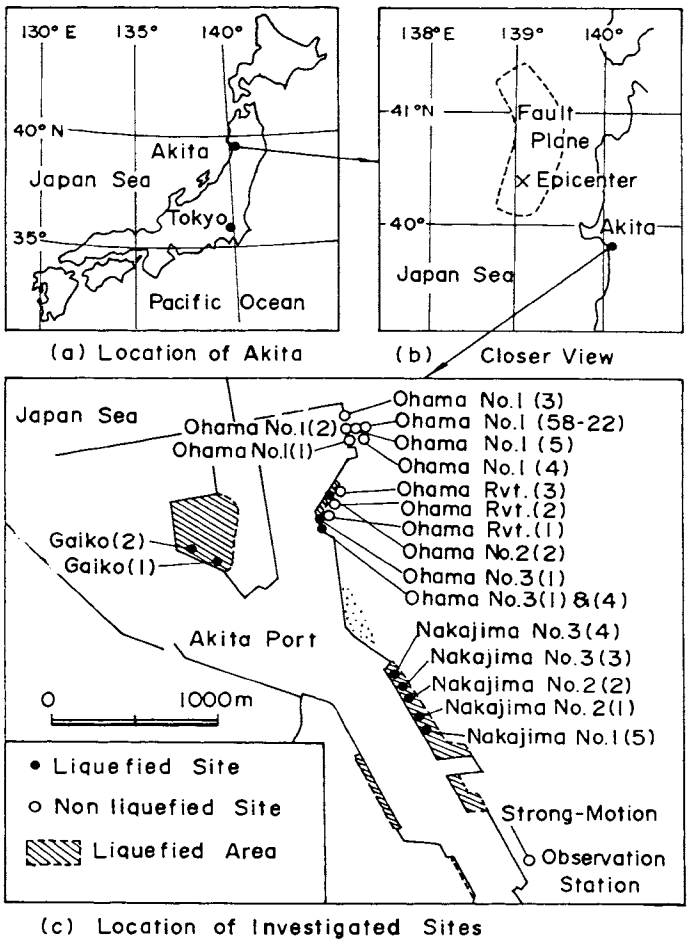

Fig. 1 Epicenter and Akita Port

Fig.2, by the multiple mechanism composed of virtual simple shear mechanisms in arbitrary orientations; each virtual simple shear mechanism is assumed to follow the hyperbolic stress-strain relation with hysteresis given by Masing's rule. This model, originally proposed by Towhata and Ishihara(1985), is modified in order to incorporate the ability to achieve realistic hysteresis loop instead of those given by Masing's rule. The approach for modifying the hysteresis loop is similar to that proposed by Ishihara et al(1985).

The main features of the model are as follows;

(1) Hysteretic damping energy consumed by drained cyclic loading at various cyclic amplitudes are consistent with the laboratory test results.
(2) Effect of principal axis rotation is taken into account.
(3) Material anisotropy can readily be incorporated into the model.

The parameters necessary for specifying the hyperbolic relation are friction angle ϕ_f and elastic shear modulus G_{ma} measured under the confining pressure of σ_{ma}'. These parameters determine the constants of the hyperbolic relation under the initial effective confining pressure of σ_{mo}' as follows;

$$\begin{aligned} \tau_{mo} &= \sigma_{mo}' \sin\phi_f \\ G_{mo} &= G_{ma} \sqrt{\sigma_{mo}'/\sigma_{ma}'} \\ \gamma_{mo} &= \tau_{mo}/G_{mo} \end{aligned} \qquad (1)$$

in which
τ_{mo} : shear strength
G_{mo} : elastic shear modulus
γ_{mo} : reference shear strain

Apart from the shear mechanism, excess pore water pressure is generated by the following rule. First of all, a state variable S is defined as a variable which is equivalent to σ_m'/σ_{mo}' under undrained condition with a constant total confining pressure. In the present model, the state variable S is determined from the shear stress ratio $r=\tau/\sigma_{mo}'$ and the liquefaction parameter S_o, to be defined as a measure of cyclic mobility, as follows (see Fig.3);

$$\begin{aligned} S &= S_o \quad (\text{if } r<r_3) \\ S &= S_2 + \sqrt{(S_o-S_2)^2 + [(r-r_3)/m_1]^2} \quad (\text{if } r>r_3) \end{aligned} \qquad (2)$$

in which
$\tau = \sqrt{\tau_{xy}^2 + [(\sigma_y'-\sigma_x')/2]^2}$
$r_2 = m_2 S_o$
$r_3 = m_3 S_o$
$S_2 = S_o - (r_2-r_3)/m_1$
$m_1 = \sin\phi_f$
$m_2 = \sin\phi_p$ (ϕ_p is phase transformation angle)
$m_3 = 0.67 m_2$

Secondly, the liquefaction parameter S_o appearing in the above equation is given by the normalized plastic shear work w (i.e. $w=W_s/W_n$, in which W_s:plastic shear work, and $W_n = (1/2)\tau_{mo}\gamma_{mo}$) as follows (see Fig.4);

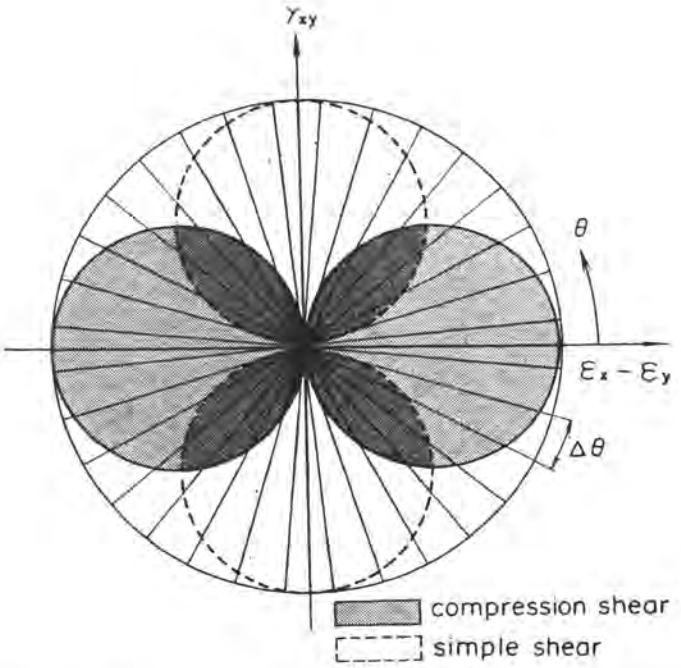

Fig. 2 Schematic figure for multiple simple shear mechanisms (pairs of circles indicate mobilized virtual shear strain in positive and negative modes of compression shear and simple shear)

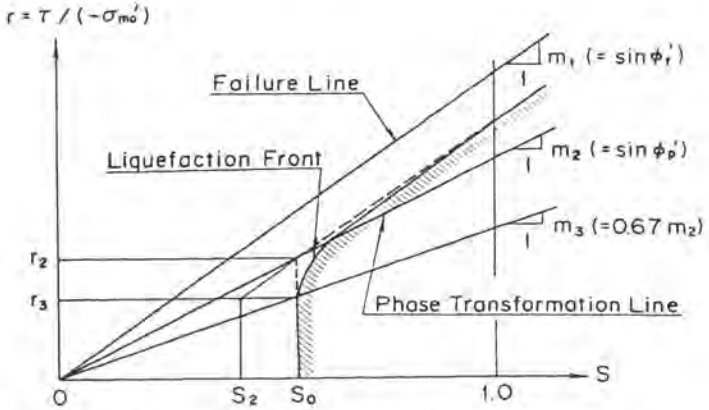

Fig. 3 Schematic figure of liquefaction front, state variable S and shear stress ratio r

$$\begin{aligned} S_o &= 1-0.6(w/w_1)^{p_1} \quad (\text{if } w<w_1) \\ S_o &= (0.4-S_1)(w_1/w)^{p_2} + S_1 \quad (\text{if } w>w_1) \end{aligned} \qquad (3)$$

The parameters necessary for the above relation are S_1, w_1, p_1, and p_2. These parameters are determined by backfitting to the test results obtained under undrained cyclic loading conditions.

When the effective stress analysis is conducted, the state variable S, given by Eq. (2), is converted into equivalent plastic volumetric strain. Moreover, in accordance with the progress of liquefaction (i.e. variation of the state variable S and the liquefaction parameters S_o), the constants of the hyperbolic relation, i.e. shear strength τ_m and elastic shear modulus G_m, are given as follows;

When $S_o > 0.4$

$$\tau_m = \tau_{mo} S, \quad G_m = \tau_m / \gamma_{mo} \tag{4}$$

When $S_o < 0.4$

$$\tau_m = \tau_{mo} S + \Delta\tau_m, \quad G_m = \tau_m / \gamma_m \tag{5}$$

in which

$\Delta\tau_m = \Delta r_m \sigma_{mo}'$

$\Delta r_m = (m_1 - m_2)(0.4 - S_o)$

$\gamma_m = \gamma_{mo} / (S_o / 0.4)$

When the initial condition for the dynamic analysis happens to give $S_o < 0.4$, some modifications are applied to the above equation. Moreover, a parameter c_1 is introduced in computing the plastic shear work as a multiplier for the elastic shear work to be subtracted from the total shear work; this makes it possible to simulate the threshold shear stress ratio for generating excess pore water pressure.

Above-mentioned formulation adds the following features to the present model;

(4) Robustness is incorporated for simulating the cyclic mobility and liquefaction by a scheme for enlarging the shear strain scale with the progress of liquefaction as indicated by Eq. (5).
(5) Liquefaction resistance, i.e. the ratio of cyclic shear stress over initial confining pressure, becomes independent of the initial confining pressure as indicated by the definition of normalized plastic shear work w.

SHEET PILE QUAYWALL, SOIL CONDITIONS and INPUT MOTIONS

The structure in Akita Port to be analyzed by the present effective stress model is a quaywall of Ohama No.2 Wharf with water depth of ten meters shown in Fig. 5. As shown in the same figure, the upper part of the steel sheet pile displaced about 1.2 meters toward sea. A crack due to bending was observed in the steel sheet pile at about four meters above the sea bed. Sand boils and settlements were observed at the apron, indicating that an excessively large bending moment acted on the sheet pile due to liquefaction of back fill sand. For more details, see Tsuchida et al, 1985.

The backfill sand and the foundation of the quaywall are, in the analysis, idealized into four kinds of soil layers as shown in Fig.5. The soil layers are further idealized into the finite element mesh as shown in Fig. 6. The parameters of the soil, shown in Table 1, are determined by the results of the seismic wave propagation survey and the laboratory data obtained under undrained cyclic loading.

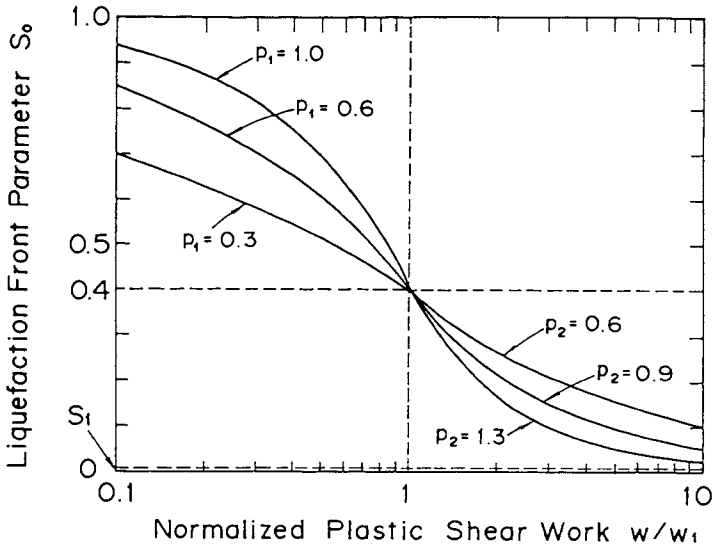

Fig. 4 Liquefaction Front Parameter

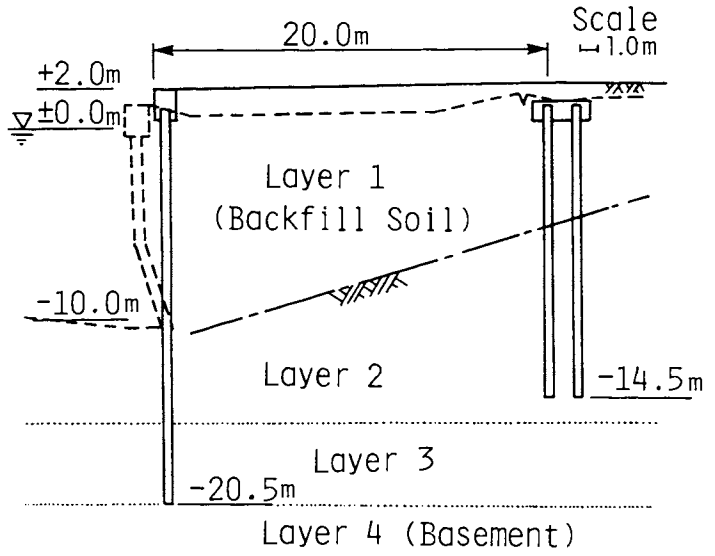

Fig. 5 Cross Section of Ohama No.2 Wharf

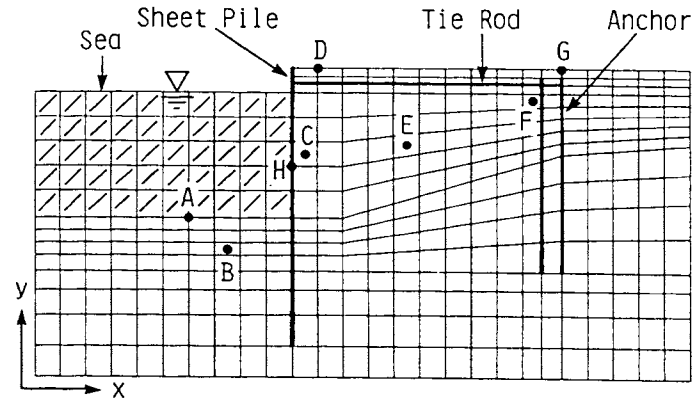

Fig. 6 Finite Element Mesh for Quaywall

As an example, by using the parameters for layer one, a soil element test (isotropically consolidated at the confining pressure of 50 kPa) under undrained cyclic loading conditions is simulated as shown in Fig. 7. As shown in this figure, typical features of the cyclic mobility are appropriately simulated. The simulation results in the liquefaction when the shear stress ratio is 0.11 and is applied 16 cycles; i.e. effective mean stress becomes almost equal to zero if the shear stress is zero, and the shear strain peak-to-peak amplitude becomes greater than 5 percent.

The soil conditions apart, the sheet pile is of FSP-VI$_L$ type, having the constants, per unit breadth of the beam, the second moment of area of 8.6 x 10^{-4} m^4, cross sectional area of 0.0306 m^2, and density of 7.5 t/m^3, and is simulated by a linear beam element. The tie rod is simulated by a beam element of which mass is assumed to be zero and is connected with the sheet pile and the anchor piles by hinges. Two of the anchor piles are idealized also by the linear beam elements of which top ends are rigidly fixed with each other. No friction is assumed to be acting between the soil and the sheet piles. The sea water is modeled as incompressible fluid and is formulated as an added mass matrix (Zienkiewicz, 1977). The side and the bottom boundaries in Fig.6 are simulated by viscous dampers.

By using the model outlined above, the behavior of the steel sheet pile quaywall, shown in Fig. 5, is numerically simulated here with the recorded earthquake motions at Akita Port. The maximum accelerations of the recorded motions at the non-liquefied site, shown in lower right hand side corner in Fig.1, are 190 and 205 Gals in NS and EW components. The earthquake motion is at first instrument corrected, deconvoluted by equivalent linear method for obtaining the incident wave, and transformed into the perpendicular direction to the face line of the quaywall as shown in Fig.8. Before the dynamic analysis, the static analysis was conducted with gravity for idealizing the initial stress acting before the earthquake. The effective stress earthquake response analysis of the free fields was also conducted before the dynamic analysis, for incorporating the realistic boundary conditions with the aid of the viscous dampers at both sides of the boundaries in Fig. 6.

The dynamic analysis of the quaywall is conducted under undrained condition (Zienkiewicz et al, 1982). The numerical integration is done by Wilson-θ method (θ=1.4) at the time step of 0.01 seconds. Rayleigh damping (α=0 and β=0.005) which is proportionally decreasing with the degree of liquefaction is used for ensure the stability of the numerical solution process.

Table 1 Parameters of sand used for the simulation

	LAYER 1	LAYER 2	LAYER 3	LAYER 4
G_{ma} (kPa)	33800	72200	74970	168200
K_a* (kPa)	89930	192100	199470	447530
σ_{ma}' (kPa)	50	110	138	157
ϕ_f (degree)	37	41	39	44
ϕ_p (degree)	30	30	--	30
s_1	0.005	0.005	--	0.005
w_1	1.8	3.2	--	4.4
p_1	0.35	0.33	--	0.37
p_2	1.0	0.76	--	0.94
c_1	1.0	1.5	--	1.5

* bulk modulus of soil skeleton

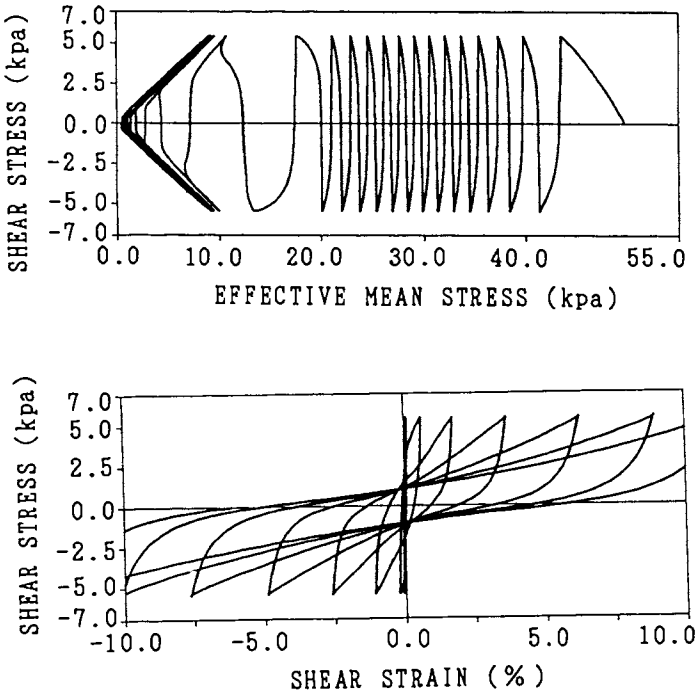

Fig. 7 Computed Undrained Cyclic Loading Test for the Soil in Layer 1

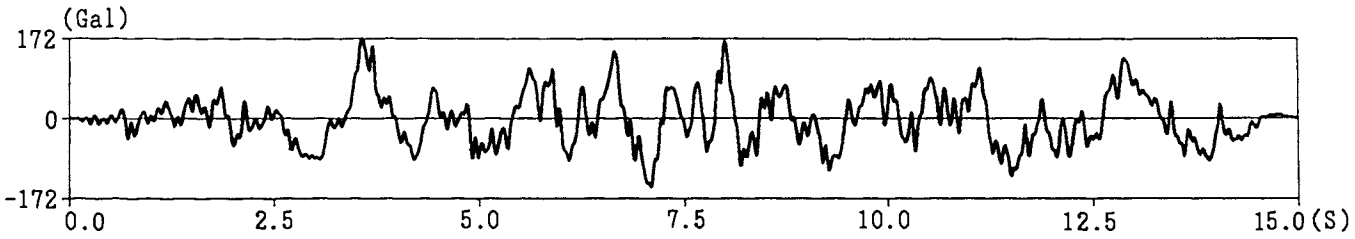

Fig. 8 Input Earthquake Motion (Incident Wave to Ohama No. 2 Wharf with Twice the Amplitude)

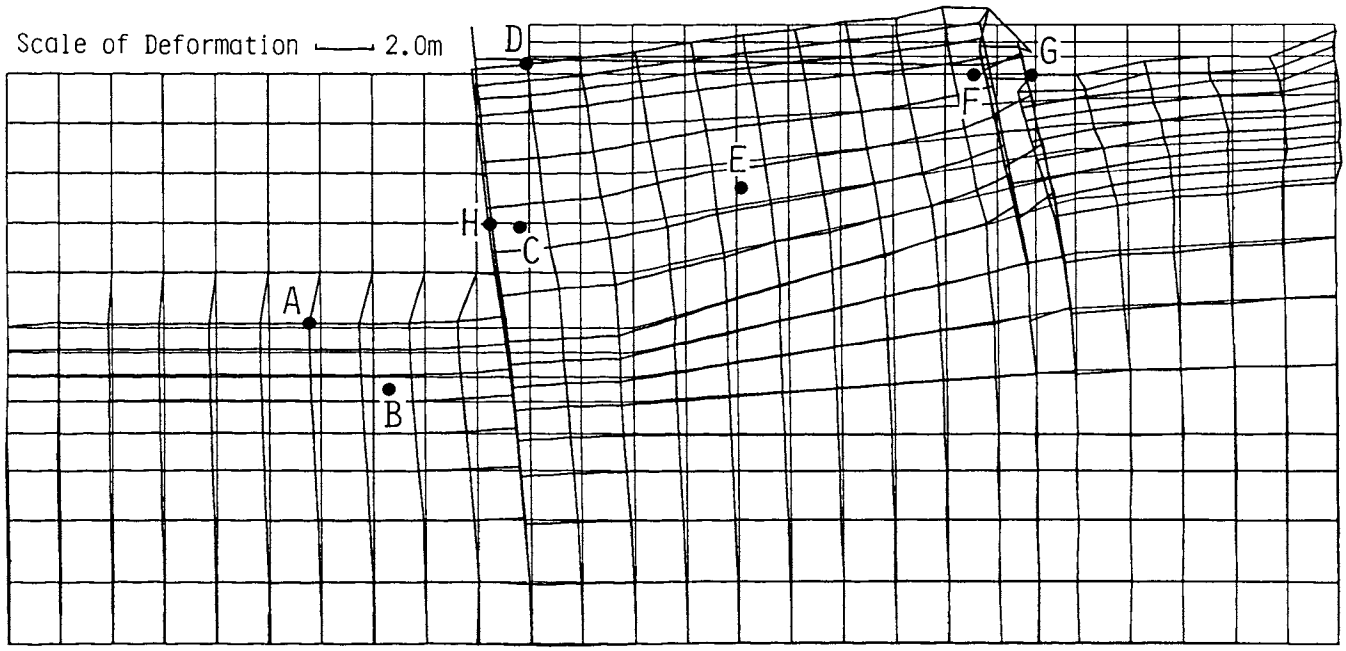

Fig. 9 Computed Deformation of Quaywall at the End of Computation (15 seconds)

RESULTS OF THE ANALYSIS

The numerical simulation, after 15 seconds of shaking, results in the deformation of the quaywall as shown in Fig. 9; the deformations towards sea are mainly recognized at the soil wedges in front of and behind the sheet pile. The maximum acceleration at the top of the quaywall is about 150 Gals as shown in Fig. 10. It is to be noted in this figure and the figures to follow, the alphabets indicate the locations shown in Fig.9. As the shaking continues, the horizontal displacements gradually increase towards sea as shown in Fig.11. The backfill soil behind the sheet pile gradually settles as shown in Fig.12 whereas the sea bed in front of the sheet pile gradually swells as shown in the same figure.

The horizontal displacement at the sheet pile is computed as 2.1 meters at the end of the shaking whereas the observed displacement was,

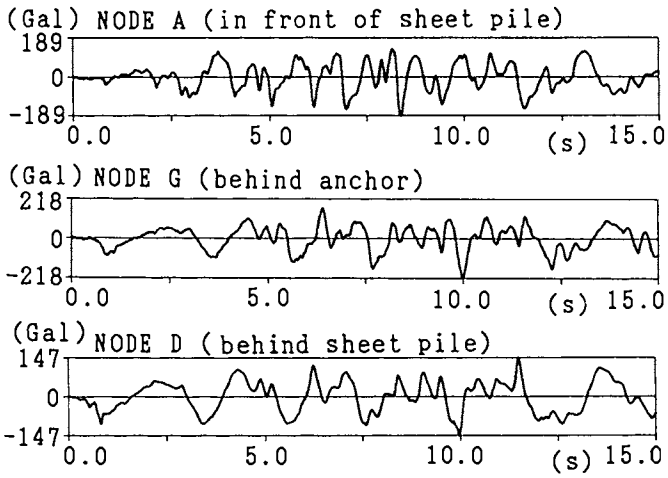

Fig.10 Horizontal Response Acceleration

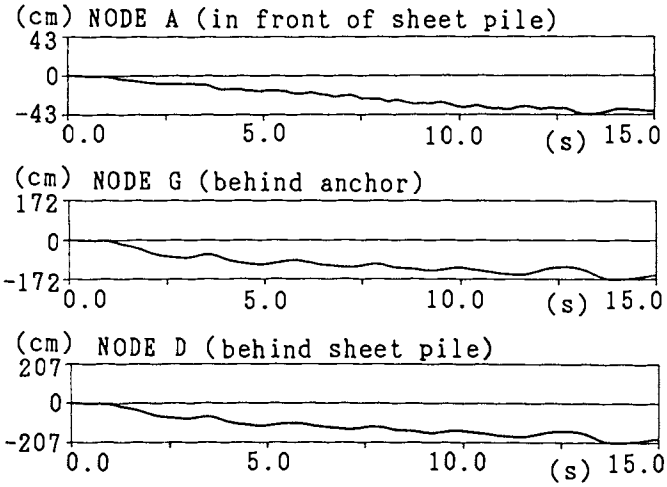

Fig. 11 Horizontal Response Displacement

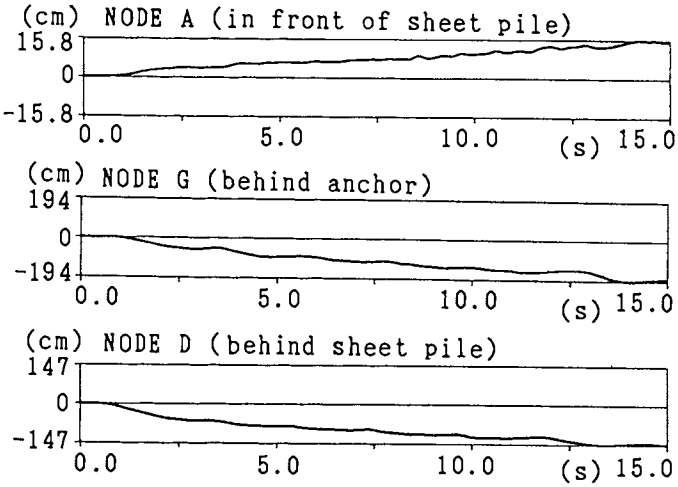

Fig. 12 Vertical Response Displacement

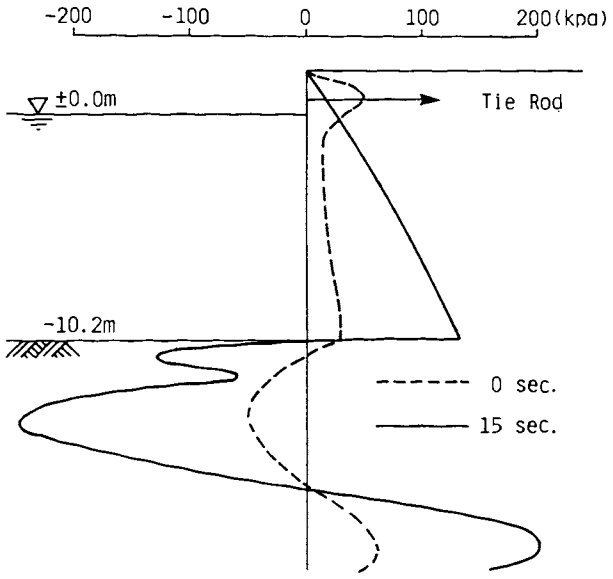

Fig. 13 Normal Stresses on Sheet Pile before and after the Earthquake

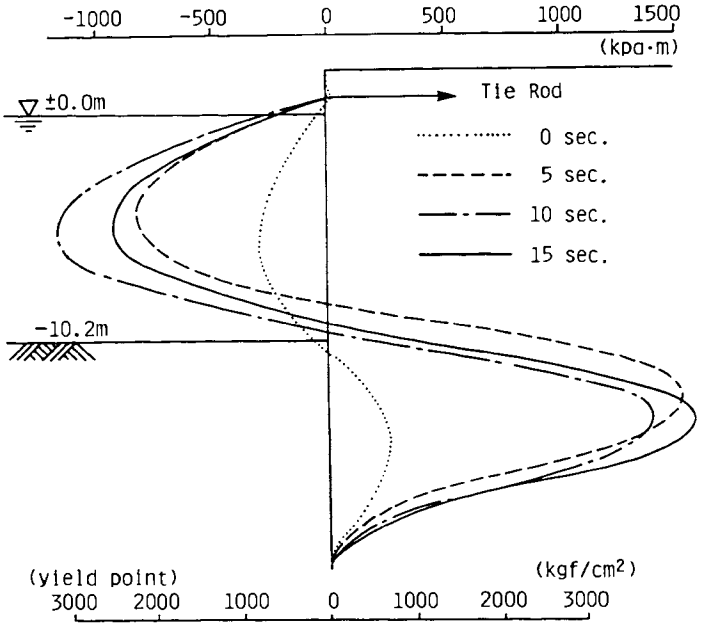

Fig. 14 Bending Moment (in upper scale) and Bending Stress (in lower scale) before and after the Earthquake

as mentioned earlier, 1.2 meters, indicating the computed displacement is as 1.8 times large as the observed one. A closer examination of the observed displacement, however, reveals that the displacement was measured relative to the temporarily fixed standard face line, which was drawn by assuming that both ends of Ohama No.2 Wharf did not displaced towards sea. It is probable, in reality, that both ends of Ohama No.2 Wharf displaced towards sea. This indicates that actual displacement is larger than 1.2 meters, being closer to the computed displacement.

The earth pressures, i.e. the normal total stresses (i.e. normal effective stresses + excess pore water pressures), acting on the sheet pile after 15 seconds of shaking, shown in Fig.13, tend to be greater greater than those before the shaking. Corresponding to those changes in the normal total stresses, the bending moment of the sheet pile changes as shown in Fig.14. The bending moment at the level of -6 meters from the water level gradually increases as shown in Fig.15.

The maximum stress due to bending is computed as 320000 kPa as shown in Fig.14 whereas the failure strength of the steel sheet pile is 300000 kPa, which is slightly less than the earthquake induced bending stress computed in the analysis. This indicates that the observed phenomenon, i.e. the failure of the sheet pile, is well explained by the analysis because, as mentioned earlier, the sheet pile is idealized with the linear beam element, which is assumed never to fail.

Excess pore water pressures in the soils in front of and behind the sheet pile are computed as shown in Fig. 16. The excess pore water pressures gradually increase behind the sheet pile as the shaking continues. However, the

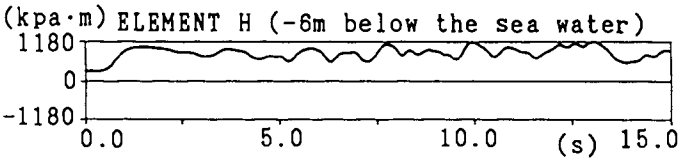

Fig. 15 Time History of Bending Moment at -6 m

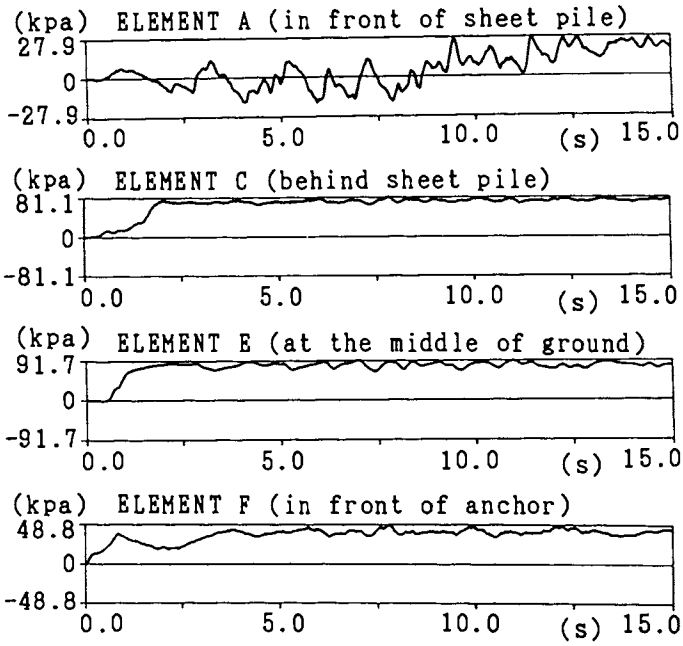

Fig. 16 Excess Pore Water Pressures

excess pore water pressures in front of the sheet pile, at first, fluctuates around zero excess pore water pressures and, as the shaking continues, gradually increase up to positive values.

Though the observed data during the earthquake are far from satisfactory, the results of the analysis presented so far indicate that the results of the analysis are not contradictory to many of the observed phenomena relevant to the deformation of the sheet pile quaywall. It is concluded that, though some modification might be still needed in the analysis, the approach taken in the present analysis is capable of representing the essential feature of the observed damage to the sheet pile quaywall during the earthquake.

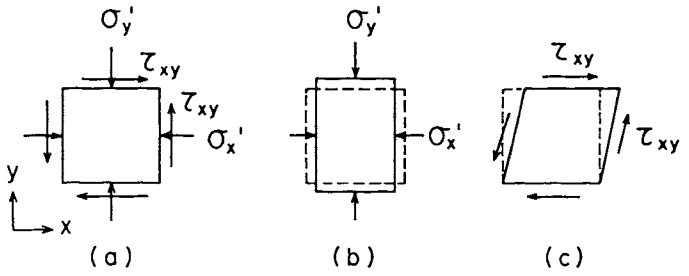

Fig.17 Schematic Figure of Shear Mechanisms

MECHANISM OF DEFORMATION

The mechanism of the above-mentioned response of the sheet pile quaywall is understood by looking into the stress-strain relations of soil elements in the ground. Obviously the constitutive model used in the present study is not simple enough to be composed of two mechanisms shown in Fig. 17; a shear mechanism between the axial stress difference ($\sigma_x'-\sigma_y'$) and the axial strain difference ($\varepsilon_x-\varepsilon_y$) and another shear mechanism between the shear stress (τ_{xy}) and the shear strain (γ_{xy}). However, it is easier to understand the shear mechanism by separately looking at them in accordance with two mechanisms shown in Fig.17. In what follows, the effective stress path, i.e. the relation between the average effective stress : $(\sigma_x'+\sigma_y')/2$ and the deviatoric stress : $\tau=\sqrt{\tau_{xy}^2+[(\sigma_x'-\sigma_y')/2]^2}$, the shear mechanism shown in Fig.17(b), and the shear mechanism shown in Fig. 17(c) will be presented for two of the soil elements which are considered representative of the ground behavior.

In front of the quaywall at the soil element B in Fig.9, the shear stress τ increases, as shown in Fig.18, just after the start of shaking and the effective confining pressure increases due to dilatancy of the sand. However, the effective confining pressure gradually decreases with decrease in the shear stress as shown in the upper most row in Fig.18. In accordance with these processes, the axial strain difference rapidly increases as shown in the middle row. The shear strain γ_{xy} gradually increases in accordance with the deformation of the sheet pile as shown in the bottom row.

Behind the sheet pile quaywall at the soil element C in Fig.9, the effective confining pressure rapidly decreases as soon as the shaking starts as shown in the upper most row in Fig.19. The corresponding to the decrease of the effective confining stress, the axial strain difference rapidly increases and the axial stress difference is released to a very low value as shown in the middle row in Fig.19. The order-of-magnitude of the shear strain γ_{xy}, as shown in the bottom row, is negligibly small in comparison with that of the axial strain difference.

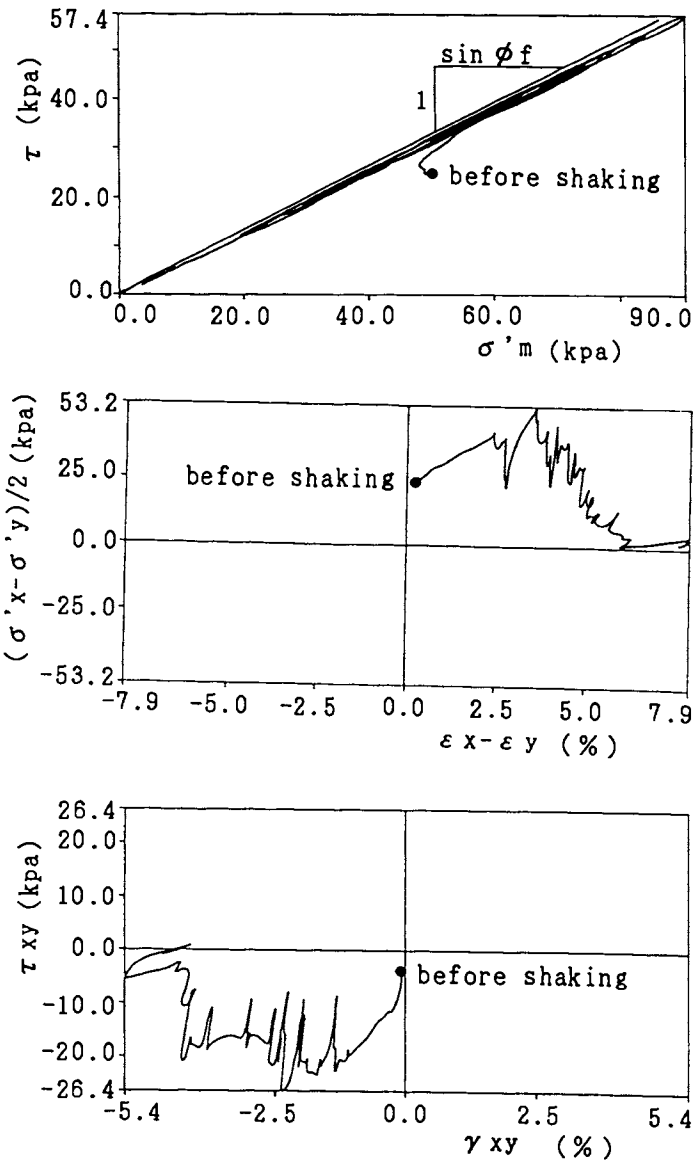

Fig. 18 Stress and Strain of Soil in front of Sheet Pile

In both of the soil elements, the strains are gradually increased due to the existence of the initial stresses and its release in accordance with the cyclic mobility. This is understood as the essential mechanism of deformation due to cyclic mobility. This mechanism of deformation is quite different from the mechanism of sliding.

CONCLUSIONS

In the present study, cyclic mobility associated damage to the sheet pile quaywall is analyzed by the effective stress model. The results of the analysis is consistent with the observed deformation and the observed yielding of the sheet pile.

The major deformations are recognized in the soil wedges in front of and behind the sheet pile. In both of the soil wedges, the strains are gradually increase due to the existence of the initial stresses and its release in accordance with the cyclic mobility. This is understood as the essential mechanism of deformation due to cyclic mobility of saturated soil-structure systems.

REFERENCES

Iai,S., "A Numerically Robust Modeling of Liquefaction and Cyclic Mobility," Seventh Conference of the International Association for Computer Methods and Advances in Geomechanics, 1991 (to be presented)

Ishihara,K., Yoshida,N. and Tsujino,S, "Modelling of Stress-Strain Relations of Soils in Cyclic Loading," Proc. 5th International Conference on Numerical Methods in Geomechanics, Nagoya, pp.373-380, 1985

Towhata,I. and Ishihara,K., "Modelling Soil Behaviour under Principal Stress Axes Rotation," Proc. 5th International Conference on Numerical Methods in Geomechanics, Nagoya, pp.523-530, 1985

Tsuchida,H. et al., "Damage to Port Structures by the 1983 Nipponkai-Chubu Earthquake," Technical Note of the Port and Harbour Research Institute No.511, p.447, 1985

Zienkiewicz,O.C., "The Finite Element Method," 3rd edition, Chapter 21, McGraw-Hill Book Co. 1977

Zienkiewicz,O.C. and Bettess,P, "Soils and Other Saturated Media under Transient, Dynamic Conditions," Soil Mechanics-Transient and Cyclic Loads. (Pande and Zienkiewicz eds.) John Wiley and Sons, pp.1-16, 1982

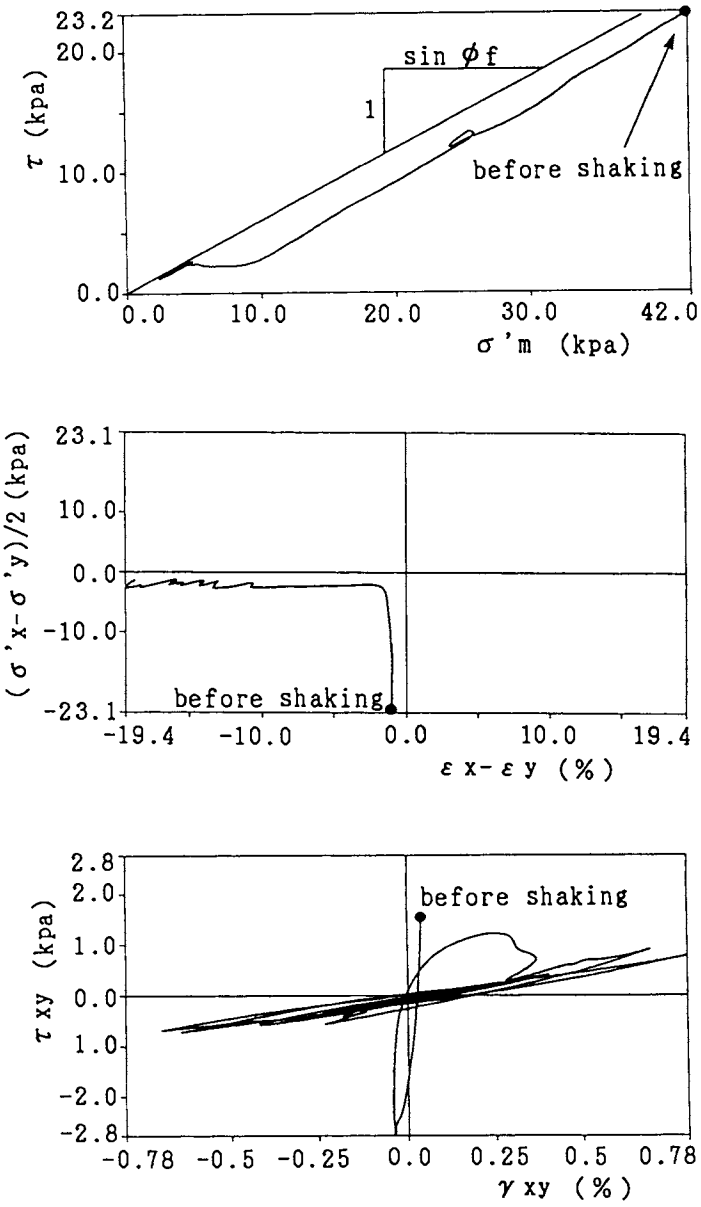

Fig. 19 Stress and Strain of Soil behind Sheet Pile